

Projected wavefunction study of Spin-1/2 Heisenberg model on the Kagome lattice

Ying Ran,¹ Michael Hermele,¹ Patrick A. Lee,¹ and Xiao-Gang Wen¹

¹*Department of Physics, Massachusetts Institute of Technology, Cambridge, Massachusetts 02139*

(Dated: November 13, 2006)

We perform a Gutzwiller projected wavefunction study for the spin-1/2 Heisenberg model on the Kagome lattice to compare energies of several spin-liquid states. The result indicates that a U(1)-Dirac spin-liquid state has the lowest energy. Furthermore, even without variational parameters, the energy turns out to be very close to that found by exact diagonalization. We show that such a U(1)-Dirac state represents a quantum phase whose low energy physics is governed by four flavors of two-component Dirac fermions coupled to a U(1) gauge field. These results are discussed in the context of recent experiments on ZnCu₃(OH)₆Cl₂.

PACS numbers: 75.10.Jm, 75.50.Ee

Recent experimental studies of a spin-1/2 Kagome system ZnCu₃(OH)₆Cl₂[1, 2, 3] show that the system is in a non-magnetic ground state. The Kagome lattice can be viewed as corner-sharing triangles in two-dimension(Fig.1(a)). The compound shows no magnetic order down to very low temperature (50mK) compared with the Curie-Weiss temperature (>200K). The spin susceptibility rises with decreasing temperature, but saturates to a finite value below 0.3 K. The specific heat is consistent with a linear T behavior below 0.5 K. There is no sign of a spin gap in dynamical neutron scattering. These observations led us to re-examine the issue of the ground state of the spin-1/2 Kagome lattice.

Based on Monte Carlo studies of Gutzwiller projected wavefunctions, we propose the ground state to be a U(1)-Dirac spin-liquid state which has relativistic Dirac spinons. The low energy effective theory is a U(1) gauge field coupled to four flavors of two-component Dirac fermions in 2+1 dimension. This state was studied earlier in the mean-field approximation[4]. However, that study focused on an instability toward a Valence Bond Solid (VBS) state which breaks translation symmetry[4]; it was not appreciated that the U(1)-Dirac state can be a stable phase. Using the Projective Symmetry Group[5, 6, 7] (PSG) technique, we reconsider the stability of the U(1)-Dirac state and find it can be stable. Our numerical calculations confirm that neighbor states like the VBS states and chiral spin-liquid state all have higher energies.

One way to construct spin-liquid states is to introduce fermionic spinon operators [8, 9] f_{\uparrow} and f_{\downarrow} to represent the bosonic spin operator: $\vec{S}_i = \frac{1}{2}f_{i\alpha}^{\dagger}\vec{\sigma}_{\alpha\beta}f_{i\beta}$. This representation enlarges the Hilbert space, and a local constraint is needed to go back to the physical Hilbert space: $f_{\uparrow}^{\dagger}f_{\uparrow} + f_{\downarrow}^{\dagger}f_{\downarrow} = 1$. For the nearest neighbor Heisenberg model

$$H = J \sum_{\langle ij \rangle} \vec{S}_i \cdot \vec{S}_j, \quad (1)$$

we can substitute the spin operator by the spinon operators, so that the spin interaction is represented as a four-fermion interaction. The four-fermion interaction

can be decomposed via a Hubbard-Stratonovich transformation by introducing the complex field χ_{ij} living on the links. The path integral of the spin model is then $Z = \int d\chi d\lambda df df^{\dagger} e^{-S}$, where the action is

$$S = \int d\tau \left[\sum_i f_{i\alpha}^{\dagger} \partial_{\tau} f_{i\alpha} + i\lambda_i (f_{i\alpha}^{\dagger} f_{i\alpha} - 1) \right. \\ \left. \sum_{ij} 2J |\chi_{ij}|^2 + J (\chi_{ij} f_{j\alpha}^{\dagger} f_{i\alpha} + h.c.) \right] \quad (2)$$

Here λ is the Lagrangian multiplier to ensure the local constraint, and it can be viewed as the time component of a compact U(1) gauge field, whereas the phase of χ_{ij} can be viewed as the space components of the same gauge field. Only when the full gauge field fluctuations are included can one go back to the physical Hilbert space.

With this fermionic representation, one can do a mean-field study of the spin-liquid states by taking χ_{ij} 's as mean-field parameters. For the Kagome lattice, the mean-field states are characterized by the fluxes through the triangles and the hexagons. Controlled mean-field studies were done by generalizing the SU(2) spin model to SU(N) spin model via introducing N/2 flavors of fermions[4, 10], and several candidate states were found:

- (i) Valence Bond Solid (VBS) states which breaks translation symmetry.
- (ii) a spin liquid state (SL- $[\frac{\pi}{2}, 0]$) with a flux $+\pi/2$ through each triangle on Kagome lattice and zero-flux through the hexagons. This is a chiral spin liquid which breaks time-reversal symmetry.
- (iii) a spin liquid state (SL- $[\pm\frac{\pi}{2}, 0]$) with staggered $\pi/2$ -flux through the triangles ($+\frac{\pi}{2}$ through up triangles and $-\frac{\pi}{2}$ through down triangles) and zero-flux through the hexagons.
- (iv) a spin liquid state (SL- $[\frac{\pi}{2}, \pi]$) with $+\pi/2$ -flux through the triangles and π -flux through the hexagons.

- (v) a uniform RVB spin liquid state (SL-[0, 0]) with zero-flux through both triangles and hexagons. This state has a spinon Fermi surface.
- (vi) a U(1)-Dirac spin liquid state (SL-[0, π]) with zero-flux through the triangles and π -flux through the hexagons. This state has four flavors of two-component Dirac fermions.

Marston and Zeng[10] found that among the spin liquid states (ii)-(v), the chiral spin liquid SL- $[\frac{\pi}{2}, 0]$ has the lowest mean-field energy. But numerical calculations[11] do not support a large chirality-chirality correlation, and Hastings[4] found SL-[0, π] to be the state with the lowest mean-field energy among the non-chiral spin liquid states. However its mean-field energy is still higher than that of (ii). All the above mean-field arguments are based on the $\frac{1}{N}$ expansion treatment of gauge fluctuation, which may fail when $N = 2$ in the physical case. To clarify which candidate is the physically low energy spin liquid state, we do a Monte Carlo study on the trial projected wavefunctions[12].

As we mentioned, fermionic representation enlarges the Hilbert space. One way to treat the unphysical states is to include gauge fluctuations. Another direct way to remove the unphysical states is to do a projection by hand. Suppose that we have a mean-field ground state wavefunction $|\Psi_{mean}(\chi_{ij})\rangle$ with mean-field parameters χ_{ij} 's, we can project out all the unphysical states, then the resulting wavefunction $|\Psi_{prj}\rangle$ would be a physical state: $|\Psi_{prj}(\chi_{ij})\rangle = P_D|\Psi_{mean}(\chi_{ij})\rangle$, where $P_D = \prod_i (1 - n_{i\uparrow}n_{i\downarrow})$ is the projection operator ensuring one fermion per site. It turns out that the calculation of energy $\langle \Psi_{prj} | H | \Psi_{prj} \rangle$ can be implemented by a Monte Carlo approach with power law complexity, which means that one can do a fairly large lattice.[12]

We note that states related by a global transformation $\chi_{ij} \rightarrow -\chi_{ij}^*$ represent the same spin wavefunction after projection. This is because projection of holes $h_{\uparrow} = f_{\downarrow}^{\dagger}$ gives the same state as projection of fermions and the hopping parameter is transformed accordingly. This is a special case of the $SU(2)$ gauge symmetry[13]. In particular, if χ_{ij} is real, the projected state and its energy are independent of a global sign change.

For spin-1/2 nearest neighbor anti-ferromagnetic Heisenberg model Eq.(1), we did the Monte Carlo calculation for energies of projected spin liquid states on lattices with 8x8 and 12x12 unit cells (each unit cell has 3 sites). We choose mixed boundary conditions; i.e., periodic along one Bravais lattice vector, and anti-periodic along the other Bravais lattice vector. The results are summarized in Table I.

We found that the U(1)-Dirac state (this state is the *projected* spin liquid of the mean-field state (vi) proposed by Hastings[4]) has the lowest energy, which is $-0.429J$ per site. Note that these results change the order of

Spin liquid	8x8x3 lattice	12x12x3 lattice
SL- $[\frac{\pi}{2}, 0]$	-0.4010(1)	-0.4010(1)
SL- $[\pm\frac{\pi}{2}, 0]$	-0.3907(1)	-0.3910(1)
SL- $[\frac{\pi}{2}, \pi]$	-0.3814(1)	-0.3822(1)
SL-[0, 0]	-0.4115(1)	-0.4121(1)
SL-[0, π]	-0.42866(2)	-0.42863(2)

TABLE I: For all candidate projected spin-liquids, we list the energy per site in unit of J . The U(1)-Dirac state SL-[0, π] is the lowest energy state, and its energy is even lower than some numerical estimates of the ground state energy(see Table II).

Method	energy per site
Exact Diagonalization[11]	-0.43
Coupled Cluster Method[14]	-0.4252
Spin-wave Variational method[15]	-0.419

TABLE II: We list the previous estimates for ground state energy in unit of J .

mean-field energies of the spin liquids (ii)-(vi), where the chiral spin liquid (ii) was found to be of the lowest energy. In Table II we list the estimates of the ground state energy by various methods. It is striking that even though the projected U(1)-Dirac state has *no variational parameter*, it has an energy which is even lower than some numerical estimates of ground state energy. Furthermore its energy is very close to the exact diagonalization result when extrapolated to large sample size. Thus we propose it to be the ground state of the spin-1/2 nearest neighbor Heisenberg model on the Kagome lattice.

Hastings[4] proposed a neighboring VBS ordered state as an instability of the U(1)-Dirac state. This state can be obtained by giving the fermions non-chiral masses. In particular, he proposed a VBS state with with a 2×2 expansion of the unit cell. The 12 hopping parameters on the boundary of the star of David (six triangles surrounding the hexagon) have amplitude χ_1 , while all other hoppings have amplitude χ_2 . Our numerical calculations show that this VBS ordered state has higher energy (see Table III), so the U(1)-Dirac state is stable against VBS ordering. Another neighbor state of the U(1)-Dirac spin liquid discussed by Hastings[4] is obtained by giving the fermions chiral masses. The resulting state is a chiral spin liquid with broken time-reversal symmetry, and has θ -flux through the triangles and $(\pi - 2\theta)$ -flux through the hexagons (if $\theta = 0$ the state goes back to the U(1)-Dirac state). In Table III we also show that non-zero θ increases the energy.

To determine whether the U(1)-Dirac state is a stable

State	8x8x3 lattice	12x12x3 lattice
U(1)-Dirac spin liquid	-0.42866(2)	-0.42863(2)
VBS state($ \chi_1/\chi_2 = 1.05$)	-0.42848(2)	-0.42844(2)
VBS state($ \chi_1/\chi_2 = 0.95$)	-0.42846(2)	-0.42846(2)
Chiral spin liquid($\theta = 0.05$)	-0.42857(2)	-0.42853(2)

TABLE III: We list the energy per site in unit of J for possible instabilities of the U(1)-Dirac spin liquid. The VBS state and the chiral spin liquid are those discussed in Ref[4](see text). One can see that both VBS order and chiral spin liquid increase the energy.

phase, we start with its effective theory

$$S = \int dx^3 \left[\frac{1}{g^2} (\varepsilon_{\lambda\mu\nu} \partial_\mu a_\nu)^2 + \sum_\sigma \bar{\psi}_{+\sigma} (\partial_\mu - ia_\mu) \tau_\mu \psi_{+\sigma} + \sum_\sigma \bar{\psi}_{-\sigma} (\partial_\mu - ia_\mu) \tau_\mu \psi_{-\sigma} \right] + \dots, \quad (3)$$

where the first term comes from integrating out some higher energy fermions, and \dots represents other terms that are generated by interaction. The massless Dirac fermions in the effective theory come from the gapless nodal spinons in the mean-field theory. The two-component Dirac spinor fields are denoted by $\psi_{\pm\sigma}$, where \pm label the two inequivalent nodes and σ the up/down spins. Also, $\bar{\psi}_{\pm\sigma} = \psi_{\pm\sigma}^\dagger \tau^3$, and the τ_μ are Pauli matrices. The massless fermions lead to an algebraic spin liquid [5, 6]. The stability of the U(1)-Dirac state can now be determined by examining the \dots terms: If \dots terms contain no relevant perturbations, then the U(1)-Dirac state can be stable.

The potential relevant terms are 16 possible gauge-invariant, spin-singlet bilinears of $\psi_{\pm\sigma}$. To see if those bilinears are generated by interaction or not, we need to study how lattice symmetries are realized in the effective theory (3). Because spinons are not gauge invariant, lattice symmetry is realized in the effective theory as a projective symmetry, described by a PSG. This means that the realization of lattice symmetry includes nontrivial gauge transformations. We find that 15 of 16 bilinears are forbidden by translation symmetry and time-reversal alone. The remaining bilinear, which is allowed by symmetry, is $\sum_{\pm,\sigma} \psi_{\pm\sigma}^\dagger \psi_{\pm\sigma}$. This term shifts the spinon Fermi level to make the ground state to have exactly one spinon per site. In this case, the lower three of six spinon bands are filled and the spinon Fermi level is exactly at the gapless nodal points. This analysis tells us that the U(1)-Dirac state is stable in mean-field theory (and also in a large- N treatment). Because not all scaling exponents are known in such an algebraic spin liquid, perturbations other than fermion bilinears could in principle lead to an instability. However, so far, the variational wavefunction analysis suggests that this is not the case and that the U(1)-Dirac state is stable.

Now we study the U(1)-Dirac spin liquid on the mean-

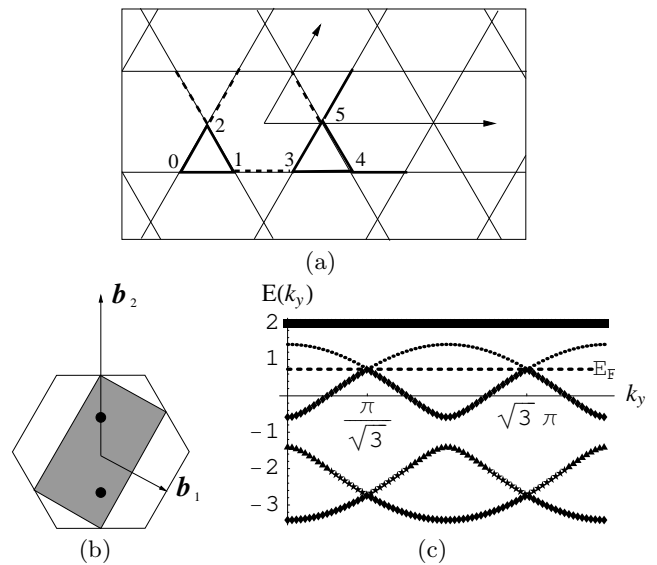


FIG. 1: (a): We choose the six-site unit cell for the Kagome lattice. The sites are labeled $0, \dots, 5$ as shown. Only those bonds depicted as bold solid lines and bold dashed lines are contained within the unit cell. The bold solid bonds have positive hopping, and the bold dashed bonds have negative hopping. (b): The Brillouin zone for the doubled unit cell (gray area), with reciprocal lattice basis vectors \mathbf{b}_i shown. The outer hexagon is the Brillouin zone for the 3-site unit cell of a single up-pointing triangle. The positions of the Dirac nodes are denoted by the black circles. (c): Plot of the band structure of the U(1)-Dirac state on the line from $\mathbf{k} = 0$ to $\mathbf{k} = \mathbf{b}_2$ with energy in units of χJ (see text). The flat band is doubly-degenerate; all others are nondegenerate. The Fermi level corresponding to one spinon per site is indicated by the dashed line.

field level. The U(1)-Dirac mean-field state is defined as the ground state of the following tight-binding spinon Hamiltonian: $H_{mean} = J \sum_{\langle ij \rangle} \chi_{ij} f_{j\alpha}^\dagger f_{i\alpha} + h.c.$. All χ_{ij} 's have the same magnitude and they produce zero-flux through the triangles and π -flux through the hexagons.

Although the U(1)-Dirac state does not break translation symmetry (because the translated state differs from the original state only by a gauge transformation), the unit cell has to be doubled to work out the mean-field spinon band structure. One can fix a gauge in which all hoppings are real as shown in Fig. 1(a). In this gauge the Dirac nodes are found to be at $\mathbf{k} = (0, \pm \frac{\pi}{\sqrt{3}a})$ as shown in Fig. 1(b)(c), where a is the Kagome unit cell spacing, i.e., twice the nearest neighbor distance. These are isotropic Dirac nodes; i.e., the Fermi velocity is the same in all directions. More nodes can be obtained by covering the momentum space by repeating the Brillouin zones. One can easily see that the Dirac nodes form a triangular lattice in momentum space with lattice spacing $\frac{2\pi}{\sqrt{3}a}$. Note that the positions of the Dirac nodes are gauge dependent, but the momentum vectors connecting any two Dirac nodes are gauge invariant. Because the

spinon excitations are gapless at the nodal points, we expect the spin-1 excitations of the U(1)-Dirac spin liquid are also gapless at zero momentum and those momenta connecting two Dirac nodes.

For the $\text{ZnCu}_3(\text{OH})_6\text{Cl}_2$ compound, the Heisenberg coupling was estimated to be $J \approx 300\text{K}$ [1], and one can calculate the Fermi velocity at mean-field level. We find that the Fermi velocity of the U(1)-Dirac ansatz is $v_F = \frac{\alpha\chi J}{\sqrt{2}\hbar}$, where χ is the magnitude of the self-consistent mean-field parameter. Hastings[4] found that $\chi = 0.221$. χ describes the renormalization of the spinon bandwidth and is not expected to be given quantitatively by the mean-field theory. Hence in the formulae below we retain χ as a parameter. We find $v_F = \frac{\alpha\chi J}{\sqrt{2}\hbar} = 19\chi \cdot 10^3$ m/s.

We can also calculate the specific heat of the U(1)-Dirac state at mean-field level. At low temperature ($k_B T \ll \chi J$), one expects a $C \propto T^2$ law because of the Dirac nodes. The coefficient is related to v_F :

$$\frac{C}{T^2} = \frac{72\zeta(3)\pi k_B^3 A}{(2\pi\hbar v_F)^2} = 1.1\chi^{-2} \cdot 10^{-3} \text{ Joule/mol K}^3, \quad (4)$$

where A is the area of the 2-D system. (Note that for $\text{ZnCu}_3(\text{OH})_6\text{Cl}_2$ compound, the unit cell spacing $a = 6.83\text{\AA}$, so $A = 2.4 \cdot 10^5$ m²/mol, where mole refers to one formula unit. We also used the fact that there are four two-component Dirac fermions.)

In a magnetic field, the spinons will form a Fermi pocket whose radius is proportional to magnetic field strength. Therefore at low temperature $k_B T \ll \mu_B B$, the specific heat is linear in T :

$$\frac{C}{T} = \frac{8\pi^3 k_B^2 A \mu_B B}{3(2\pi\hbar v_F)^2} = 0.23\chi^{-2} B \cdot 10^{-3} \text{ Joule/mol K}^2,$$

where magnetic field B is in unit of Tesla. We also find in the temperature range $\mu_B B \ll k_B T \ll \chi J$,

$$C = \frac{24\pi A k_B^3 T^2}{(2\pi\hbar v_F)^2} \left[3\zeta(3) + \frac{2\ln 2}{3} \left(\frac{\mu_B B}{k_B T} \right)^2 + O(B^4) \right].$$

Keeping the lowest order correction, the specific heat has a *temperature independent* increase proportional to B^2 .

$$\begin{aligned} \Delta C &= \frac{16\pi \ln 2 k_B A}{(2\pi\hbar v_F)^2} (\mu_B B)^2 \\ &= 6.3\chi^{-2} B^2 \cdot 10^{-5} \text{ Joule/mol K}. \end{aligned} \quad (5)$$

This is in contrast to the specific heat shift of a local moment, which decreases with T as B^2/T^2 . Eq.(5) provides a way to separate the Dirac fermion contribution from that of impurities and phonons.

The gauge field also gives a T^2 contribution to the specific heat. However, in a large- N treatment this will be down by a factor of $1/N$ compared to the fermion contribution. Furthermore, the self energy correction due to gauge fluctuations does not lead to singular corrections

to the Fermi velocity[16], so the T^2 dependence of C is a robust prediction.

We notice that experiment observed that the specific heat of Kagome compound $\text{ZnCu}_3(\text{OH})_6\text{Cl}_2$ behaves as $C \propto T^{2/3}$ in zero magnetic field over the temperature window $106 \text{ mK} < T < 600 \text{ mK}$ [1], which is enhanced from $C \propto T^2$ law. This enhancement is suppressed by a modest magnetic field[1]. Furthermore, over a large temperature range (10K to 100K), the spin susceptibility is consistent with Curie's law with 6% impurity local moment. We propose that these impurity spins (possibly due to Cu located on the Zn sites) may be coupled to the spinons to form a Kondo type ground state with a Kondo temperature $\lesssim 1\text{K}$, thus accounting for the large C/T and the saturation of the spin susceptibility below 0.3K. The Kondo physics of impurities coupled to Dirac spinons is in itself a novel problem worthy of a separate study. Meanwhile it appears to dominate the low temperature properties and obscure the true excitations of the Kagome system. We propose that a better place to look for the Dirac spectrum may be at higher temperature (above 10K) and as a function of magnetic field, where the impurity contributions may be suppressed and the unique signature of Eq.(4) and Eq.(5) may be tested. On the other hand, we caution that from Fig.1(c), the spinon spectrum deviates from linearity already at a relatively low energy scale ($\sim 0.5\chi J$). Our theory also predicts a linear T spin susceptibility of $k_B T \ll \chi J$. Knight shift measured by Cu NMR is the method of choice to separate this from the impurity contribution.

Finally we remark on a possible comparison with exact diagonalization studies which found a small spin gap of $\sim \frac{J}{20}$ and a large number of low energy singlets[11]. It is not clear whether these results can be reconciled with a U(1)-Dirac spin liquid. Here we simply remark that in a finite system the Dirac nodes can easily produce a small triplet gap and that the gauge fluctuations may be responsible for low energy singlet excitations.

We thank J. Helton and Y. S. Lee for helpful discussions. This research is supported by NSF grant No. DMR-0433632 and DMR-0517222.

-
- [1] J. S. Helton *et al.*, cond-mat/0610539.
 - [2] O. Ofer *et al.*, cond-mat/0610540.
 - [3] P. Mendels *et al.*, cond-mat/0610565.
 - [4] M. B. Hastings, Phys. Rev. B **63**, 014413 (2000).
 - [5] X.-G. Wen, Phys. Rev. B **65**, 165113 (2002).
 - [6] M. Hermele, T. Senthil, M. P. A. Fisher, P. A. Lee, N. Nagaosa, and X.-G. Wen, Phys. Rev. B **70**, 214437 (2004).
 - [7] Y. Ran and X.-G. Wen, cond-mat/0609620.
 - [8] G. Baskaran, Z. Zou, and P. Anderson, Solid State Commun. **63**, 973 (1987).
 - [9] G. Kotliar and J. Liu, Phys. Rev. B **38**, 5142 (1988).
 - [10] J. Marston and C. Zeng, J. Appl. Phys. **69**, 5962 (1991).
 - [11] C. Waldtmann *et al.*, Eur. Phys. Jour. B **2**, 501 (1998).

- [12] C. Gros, *Annals of Physics* **189**, 53 (1989).
- [13] P. Lee, N. Nagaosa, and X.-G. Wen, *Rev. Mod. Phys.* **78**, 17 (2006).
- [14] D. J. J. Farnell, R. F. Bishop, and K. A. Gernoth, *Phys. Rev. B* **63**, 220402 (2001).
- [15] L. Arrachea, L. Capriotti, and S. Sorella, *Phys. Rev. B* **69**, 224414 (2004).
- [16] D. H. Kim, P. A. Lee, and X.-G. Wen, *Phys. Rev. Lett.* **79**, 2109 (1997).